Analyst

ROYAL SOCIETY OF CHEMISTRY

PAPER

View Article Online
View Journal | View Issue

Cite this: *Analyst*, 2022, **147**, 2828

A novel AIE fluorescent probe for the monitoring of aluminum ions in living cells and zebrafish†

Yabing Gan,[b] Guoxing Yin,[b] Jianhua Wang*[a] and Peng Yin *[b]

Received 29th March 2022,
Accepted 5th May 2022

DOI: 10.1039/d2an00543c

rsc.li/analyst

A novel fluorescent probe BTD with aggregation induced emission (AIE) characteristics for the monitoring of Al^{3+} was developed. This fluorescent probe could be used to detect Al^{3+} in aqueous solution under mild conditions, along with high sensitivity and high selectivity. The detection limit of the probe BTD for Al^{3+} is as low as 3.25 nM, which is below the WHO recommendation concentration (7.41 μM) for drinking water. Furthermore, this probe was successfully applied to the sensing of Al^{3+} in living cells and zebrafish.

Introduction

Aluminum, the third most abundant element on the Earth's crust, is widely used in daily life, such as in utensils, food additives, building equipment, water purification, and pharmaceutical products.[1–3] However, as a non-essential toxic element in the biological system, the accumulation of excessive Al^{3+} could induce various diseases, including Parkinson's disease, Alzheimer's disease, and amyotrophic lateral sclerosis.[4–9] Moreover, the water-soluble Al^{3+} resulted by acid rain could cause serious damage to growing plants and the environment.[10–12] Therefore, the development of an effective method to trace Al^{3+} is of great significance to human health and environment protection.

Though traditional analysis and detection techniques, such as chromatography, spectroscopy, and electrochemical analysis, are available to detect heavy transition metal ions, they are not convenient for the analysis of plentiful samples because of expensive equipment, high cost and time-consuming procedures.[13–19] By contrast, significant progress has been achieved in the development and application of fluorescent probes for the selective binding and identification of different metals, exhibiting unique properties including operational simplicity, low cost, high sensitivity and high selectivity.[20,21] Until now, some fluorescent probes for detecting Al^{3+} have been reported based on internal charge transfer (ICT),[22–24] photo-induced electron transfer (PET),[25–29] chelation-enhanced fluorescence (CHEF),[30–32] and fluorescence resonance energy transfer (FRET) mechanisms.[33] However, most of these probes need to be applied in the organic/water mixture for the detection of Al^{3+}; the Al^{3+} ion easily dissolves in water medium. The poor water-solubility of these reported probes hinders their further application in environmental and biological systems. In recent years, fluorescent probes displaying aggregation-induced emission (AIE) characteristics have attracted great attention, and a lot of practical applications have been realized.[34–40] Hence, it is valuable to develop new AIE probes with high selectivity and high sensitivity for the quantification and bioimaging of Al^{3+}.

In this work, we rationally design and develop a novel fluorescent probe BTD with AIE characteristics, which exhibits fluorescence 'turn-on' for Al^{3+} in almost pure water (Scheme 1). This probe exhibits high sensitivity and high selectivity for the monitoring of Al^{3+} in water samples. Furthermore, the probe was successfully applied to detect Al^{3+} in BEL-7402 cells and zebrafish.

Experimental

General information

The chemicals and solvents were purchased from Aladdin (Shanghai, China) and used without further purification. TLC analysis was performed using precoated silica plates. UV–vis absorption spectra were obtained on a UV-2450 spectrophotometer (Shimadzu Co., Japan). All the experimental pure water was obtained from a Millopore-Q water ultrapurification

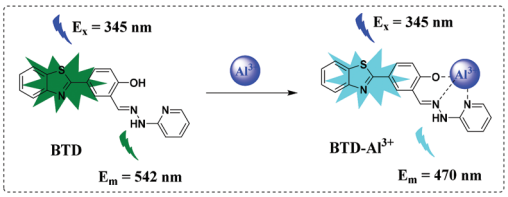

Scheme 1 Proposed mechanism for sensing Al^{3+}.

[a]*Changsha Hospital of Hunan Normal University, The Fourth Hospital of Changsha, Changsha 410081, China. E-mail: wjhcssyy@163.com*
[b]*College of Chemistry and Chemical Engineering, Hunan Normal University, Changsha 410081, China. E-mail: yinpeng@hunnu.edu.cn*
† Electronic supplementary information (ESI) available. See DOI: https://doi.org/10.1039/d2an00543c

system. ^{1}H NMR and ^{13}C NMR spectra were obtained with tetramethyl silane (TMS) as the internal standard on a BRUKER AVANCE-500 spectrometer and the chemical shifts (δ) were expressed in ppm and coupling constants (J) were in Hertz. The IR spectrum was recorded on a NEXUS with KBr pellets and reported in cm^{-1}. Mass analyses were performed using a Waters Q-Tof Premier mass spectrometer with an ESI ion source (Waters QTOF Premier, U.S.A.). Cells were imaged using a fluorescence confocal microscope (Zeiss LSM 880, Germany). Zebrafish experiments were conducted on a fluorescence confocal microscope system (Leica SP8, Germany).

General procedure for UV-visible spectroscopy and fluorescence measurements

The stock solution of probe BTD (1.0 mM) was prepared in DMSO. Stock solutions (10.0 mM) of various metal ions including Na^{+}, K^{+}, Li^{+}, Ag^{+}, Ba^{2+}, Ca^{2+}, Co^{2+}, Zn^{2+}, Mg^{2+}, Mn^{2+}, Pb^{2+}, Cd^{2+}, Cu^{2+}, Sn^{2+}, Fe^{2+}, Fe^{3+}, Cr^{3+}, Bi^{3+}, Ni^{2+}, Zr^{4+}, Ge^{4+}, Cys, Hcy, GSH, S^{2-}, SO_3^{2-}, Gly, Glu, Met, Asp, Thr, Lys, Try, and His were prepared in deionized water. These stock solutions were further diluted to the required concentration for measurement. Test solutions were prepared as follows: 20 μL of BTD solution (1.0 mM) and appropriate amounts of analyte solution were added into a test tube, and the solution was diluted to 2 mL with pure water. All the absorption and fluorescence spectra were obtained at room temperature after shaking well.

Synthesis of 4-(benzo[*d*]thiazol-2-yl)phenol (1)

To a solution of 150 mL anhydrous DMF were added 2-aminobenzenethiol (18.78 g, 150 mmol) and 4-hydroxybenzaldehyde (18.32 g, 150 mmol); then, sodium pyrosulfite (24.52 g, 129 mmol) was added to the resulting solution. The mixture was refluxed for 4 h with stirring until no starting materials were indicated by TLC. The reaction mixture was cooled to room temperature, and then poured into 1 L of cold water, and a white solid was precipitated. Then the solid was filtered and dried under vacuum to yield the target compound **1** (28.8 g, 84.5%). ^{1}H NMR (500 MHz, DMSO-d_6) δ 10.22 (s, 1H), 8.07 (d, J = 8.0 Hz, 1H), 7.98 (d, J = 8.2 Hz, 1H), 7.93 (d, J = 8.6 Hz, 2H), 7.49 (t, J = 7.6 Hz, 1H), 7.39 (t, J = 7.6 Hz, 1H), 6.94 (dd, J = 8.9, 2.5 Hz, 2H). ^{13}C NMR (126 MHz, DMSO-d_6) δ 167.9, 161.0, 154.2, 134.6, 129.5, 126.9, 125.4, 124.5, 122.8, 122.6, 116.6.

Synthesis of 5-(benzo[*d*]thiazol-2-yl)-2-hydroxybenzaldehyde (2)

To a solution of 4-(benzo[*d*]thiazol-2-yl) phenol (5.00 g, 22 mmol) in trifluoroacetic acid (120 mL) was added hexamethylenetetramine (3.70 g, 26.4 mmol); then the mixture was refluxed for 5 h. After the reaction mixture was cooled to room temperature, hydrochloric acid (100 mL, 6 mol L^{-1}) was added, and the organic layer was separated out. The aqueous layer was extracted with CH_2Cl_2 (3 × 10 mL). Then the combined organic layers were washed with brine, dried with anhydrous Na_2SO_4 and concentrated under vacuum. The crude product was purified by column chromatography to yield a white solid (1.80 g, 32%). ^{1}H NMR (500 MHz, $CDCl_3$) δ 11.27 (s, 1H), 10.03 (s, 1H), 8.35 (d, J = 2.3 Hz, 1H), 8.22 (dd, J = 8.7, 2.3 Hz, 1H), 8.05 (d, J = 8.1 Hz, 1H), 7.91 (dd, J = 8.0, 1.3 Hz, 1H), 7.53–7.48 (m, 1H), 7.42–7.38 (m, 1H), 7.12 (d, J = 8.8 Hz, 1H). ^{13}C NMR (126 MHz, $CDCl_3$) δ 196.4, 166.0, 163.5, 154.0, 135.7, 134.8, 132.8, 126.6, 126.1, 125.3, 123.1, 121.7, 120.7, 118.6.

Synthesis of the probe BTD

To a solution of 10 mL ethanol were added 5-(benzo[*d*]thiazol-2-yl)-2-hydroxybenzaldehyde (300 mg, 1.18 mmol) and 2-hydrazinylpyridine (128 mg, 1.18 mmol). The resulting mixture was stirred overnight at room temperature. Then the residue was filtered and washed with cold ethanol three times. The solid was purified by column chromatography to yield the desired probe (291 mg, 71.5%). ^{1}H NMR (500 MHz, DMSO-d_6) δ 11.10 (d, J = 26.6 Hz, 2H), 8.44–8.32 (m, 2H), 8.15 (dd, J = 5.0, 1.8 Hz, 1H), 8.11 (d, J = 7.9 Hz, 1H), 8.03 (d, J = 8.0 Hz, 1H), 7.92 (dd, J = 8.5, 2.4 Hz, 1H), 7.72–7.66 (m, 1H), 7.56–7.49 (m, 1H), 7.47–7.39 (m, 1H), 7.13 (d, J = 8.3 Hz, 1H), 7.07 (d, J = 8.5 Hz, 1H), 6.80 (dd, J = 7.2, 4.9 Hz, 1H). ^{13}C NMR (126 MHz, DMSO-d_6) δ 167.6, 158.9, 156.8, 154.2, 148.5, 138.6, 137.1, 134.7, 129.1, 127.0, 125.8, 125.5, 125.0, 122.9, 122.7, 122.1, 117.4, 115.7, 106.8.

Cell imaging studies

The BEL-7402 cells were cultured in Dulbecco's modified Eagle's medium (DMEM, GIBCO) supplemented with 10% heat-inactivated fetal bovine serum (FBS, GIBCO), streptomycin (100 μg mL^{-1}) and penicillin (100 μg mL^{-1}). The cells were seeded into a 96 well culture plate and grown in DMEM medium under a humid atmosphere of 5% CO_2 at 37 °C for 24 h. Subsequently, the cells were washed thrice with sterile phosphate buffered saline (PBS). For the detection of Al^{3+} in living cells, BEL-7402 cells were incubated with 2.0 μM probe BTD in DMEM at 37 °C for 30 min and subsequently incubated with $Al_2(SO_4)_3{\cdot}18H_2O$ (0.1, 0.2 and 0.4 mM) for 30 min, respectively, and then washed with phosphate-buffered saline (PBS) three times. Cells were imaged using a fluorescence confocal microscope (Zeiss LSM 880, Germany). (λ_{ex} = 405 nm, λ_{em} = 421–475 nm for the blue channel; λ_{ex} = 458 nm, λ_{em} = 500–550 nm for the green channel). Scale bar: 50 μm.

Zebrafish confocal fluorescence imaging

For the detection of Al^{3+} *in vivo*, 3-day-old zebrafish was used for these experiments. All animal procedures were performed in accordance with the guidelines and approved by the Animal Ethics Committee (Hunan Normal University). Zebrafish was fed with E3 embryo media (15 mM NaCl, 0.5 mM KCl, 1 mM $MgSO_4$, 1 mM $CaCl_2$, 0.15 mM KH_2PO_4, 0.05 mM Na_2HPO_4, 0.7 mM $NaHCO_3$, 10^{-5}% methylene blue; pH 7.5) at 28 °C for 30 min, then incubated with Al^{3+} (10, 20 and 50 μM, 60 min) respectively, and finally incubated with the probe (5 μM) for 60 min. All the fishes were terminally anaesthetized using MS222, and images were obtained on a fluorescence confocal microscope system (Leica SP8, Germany). (λ_{ex} = 405 nm, λ_{em} = 440–500 nm for the blue channel; λ_{ex} = 488 nm, λ_{em} = 510–550 nm for the green channel). Scale bar: 0.5 mm.

Results and discussion

Aggregation-induced emission (AIE) of the probe BTD

The probe BTD was easily synthesized, as shown in Scheme 2, *via* a three-step process. The probe and intermediates were characterized by ^{1}H NMR and ^{13}C NMR (Fig. S13–S18†). Firstly, the AIE behavior of the probe in the presence of Al^{3+} was verified by obtaining the fluorescence spectra of the probe BTD with Al^{3+} in mixed solvents with varied acetone-to-H_2O ratios. In pure acetone, almost no fluorescence was observed under excitation at 345 nm (Fig. 1). After the addition of water, the phenolic hydroxyl group, the N atoms on the pyridine and the C=N double bond have a unique affinity for Al^{3+} ions, resulting in the aggregation of the probe BTD, and the fluorescence intensities were gradually increased at 470 nm. The fluorescence intensity at 470 nm was enhanced with the increase in water content. And the content of 99% water leads to a *ca.* 49-fold increment in the fluorescence intensity. The changes in blue fluorescence could be obviously observed under UV light (Fig. 1, insert). These results suggested that the probe BTD was an AIE-active probe for the sensing of Al^{3+} ions.

Spectroscopic response

Next, we examined the responses of the probe BTD (10 μM) in pure water (containing 1% DMSO) toward Al^{3+} at 37 °C. As shown in Fig. S1,† upon the addition of 100 μM Al^{3+}, the initial absorption peak at 321 nm shifted to 327 nm. Meanwhile, the fluorescence spectrum of the probe BTD exhibited a weak fluorescence at 542 nm. After the probe was treated with 100 μM Al^{3+}, a significant fluorescence increment was observed at 470 nm by more than 338 times when excited at 345 nm, accompanied by a clear color change from green to blue (inset images of Fig. S1†). Using quinoline sulfate in 0.1 M H_2SO_4 aqueous solution as the standard, the fluorescence quantum yield was calculated to be 0.157. These results demonstrated that the probe BTD was a visual and fluorescence turn-on probe for the detection of Al^{3+} in pure water.

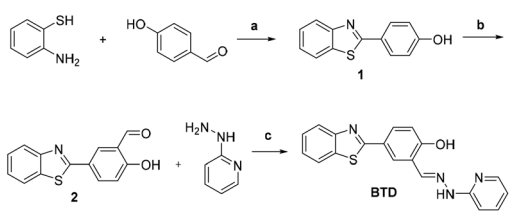

Scheme 2 Synthesis of the probe BTD. Reagents and conditions: (a) DMF, $Na_2S_2O_5$ reflux; 84.5%; (b) CF_3COOH, HMTA, reflux; 32%; (c) EtOH, at room temperature; 71.5%.

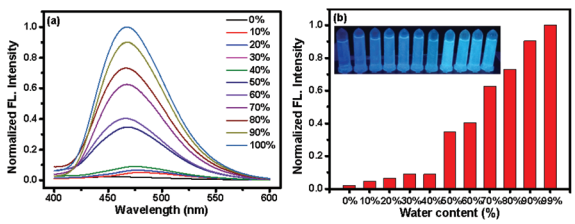

Fig. 1 (a) Normalized fluorescence spectra of the probe BTD (10 μM) in the presence of Al^{3+} (100 μM) in different water contents from 0% to 100%. (b) The corresponding normalized fluorescence intensity changes at 470 nm. λ_{ex} = 345 nm, silt: 2.5/2.5. The inset photos indicated the color changes of the probe BTD (10 μM) in the presence of Al^{3+} (100 μM) in different water contents (0–100%) under a UV lamp at 365 nm, respectively.

Time-dependence and pH effect

The response time of the probe BTD with Al^{3+} in pure water (containing 1% DMSO) was also investigated. Upon addition of Al^{3+}, the fluorescence at 470 nm increased rapidly and reached equilibrium after 25 minutes (Fig. S2†). Therefore, subsequent experiments for the monitoring of different analytes with the probe BTD were conducted for 25 min. Subsequently, the pH effect of the probe BTD for the monitoring of Al^{3+} was observed. As shown in Fig. S3,† the fluorescence of the probe BTD remained the same in the pH range of 2–10, indicating that the probe BTD was stable in a wide pH range. However, in the presence of Al^{3+}, it showed significant fluorescence enhancements at pH 2–10. Thus, the probe BTD can be used for the detection of Al^{3+} over a wide pH range, including a physiologically relevant pH value, which is favorable for its biological applications in living cells and *in vitro*.

Titration experiments

To evaluate the sensing ability of the probe BTD for Al^{3+}, fluorescence titration experiments were conducted. As shown in Fig. 2, the fluorescence at 470 nm enhanced gradually after the addition of Al^{3+} (0–10 μM). A good linear relationship was obtained in the Al^{3+} concentration range of 0–10 μM. And the detection limit of the probe BTD for Al^{3+} was calculated to be as low as 3.25 nM based on the signal-to-noise ratio (S/N = 3), which is as low as 7.41 μM Al^{3+} for bottled drinking water according to the World Health Organization (WHO) guidelines. Compared to some reported probes for Al^{3+} (Table S1†), this probe exhibited high sensitivity. These results indicated that the probe BTD is sensitive for the detection of Al^{3+} in environmental and biological systems.

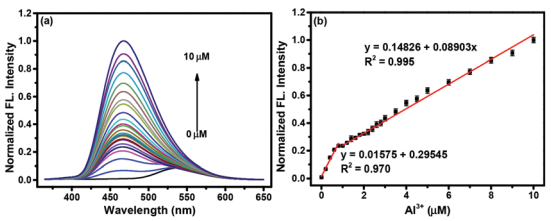

Fig. 2 (a) Normalized fluorescence intensity spectra of the probe BTD (10 μM) in the presence of 0–10 μM Al^{3+} in pure water (containing 1% DMSO). (b) The linear changes in the normalized fluorescence intensity at 470 nm of the probe BTD and as a function of Al^{3+} concentration. λ_{ex} = 345 nm, slit (nm): 2.5/2.5.

Selectivity and anti-interference

Subsequently, the selectivity of the probe BTD toward Al^{3+} was evaluated. Water-soluble metal species were tested, including Na^+, K^+, Li^+, Ag^+, Ba^{2+}, Ca^{2+}, Co^{2+}, Zn^{2+}, Mg^{2+}, Mn^{2+}, Pb^{2+}, Cd^{2+}, Cu^{2+}, Sn^{2+}, Fe^{2+}, Fe^{3+}, Cr^{3+}, Bi^{3+}, Ni^{2+}, Zr^{4+} and Ge^{4+}. As shown in Fig. 3, among these analytes, only Al^{3+} could induce a significant fluorescence enhancement, while no fluorescence was observed for the other competing analytes. Competition experiments were carried out in the presence of various metal ions and Al^{3+} under the same conditions (Fig. S4†). The fluorescence changes of the probe solution caused by the coexistence of other ions with Al^{3+} and the presence of Al^{3+} alone are similar, except for Co^{2+}, Cu^{2+}, Sn^{2+}, Fe^{2+}, Fe^{3+} and Ni^{2+}, which could slightly reduce the fluorescence intensity at 470 nm. These results demonstrated that the probe BTD had good selectivity and anti-interference ability for the detection of Al^{3+} and has the potential for monitoring Al^{3+} in complex systems.

Reversibility

Reversibility and regeneration are also essential factors for the development of devices for sensing analytes in practical applications.[41–53] We first evaluated the fluorescence response of the *in situ* product BTD-Al^{3+} toward other analytes, such as Cys, Hcy, GSH, S^{2-}, SO_3^{2-}, Gly, Glu, Met, Asp, Thr, Lys, Try, and His. As shown in Fig. S5,† fluorescence at 470 nm was significantly quenched only after Lys was added to the solution of the product BTD-Al^{3+}. However, negligible fluorescence changes were observed for other analytes under the same conditions. Subsequently, the fluorescence intensity of the solution of the product BTD-Al^{3+} was rapidly quenched for 2 min upon addition of 500 μM Lys (Fig. S6†). As shown in Fig. S7,† the alternate addition of a constant amount of Al^{3+} (50 μM) and Lys (500 μM) to the aqueous solution of probe BTD would result in switchable changes in the fluorescence intensity at 470 nm. And this reversible fluorescence interconversion could be repeated more than 4 times by the modulation of the Al^{3+}/Lys addition. These results indicated that the probe BTD could be applied to the reversible detection of Al^{3+} in environment and biological systems. In addition, the probe–Al^{3+} complex could be used to detect lysine (Fig. S8†).

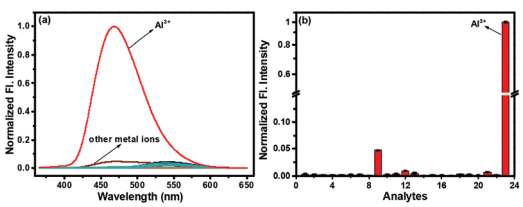

Fig. 3 (a) Normalized fluorescence spectra responses of the probe BTD (10 μM) to various metal ions in pure water (containing 1% DMSO). (b) The corresponding normalized fluorescence intensity changes at 470 nm. Various metal ions (100 μM) including: 1. None; 2. Na^+; 3. K^+; 4. Li^+; 5. Ag^+; 6. Ba^{2+}; 7. Ca^{2+}; 8. Co^{2+}; 9. Zn^{2+}; 10. Mg^{2+}; 11. Mn^{2+}; 12. Pb^{2+}; 13. Cd^{2+}; 14. Cu^{2+}; 15. Sn^{2+}; 16. Fe^{2+}; 17. Fe^{3+}; 18. Cr^{3+}; 19. Bi^{3+}; 20. Ni^{2+}; 21. Zr^{4+}; 22. Ge^{4+}; 23. Al^{3+}. λ_{ex} = 345 nm, slit (nm): 2.5/2.5.

Sensing mechanism

The sensing mechanism of the probe BTD toward Al^{3+} was carefully investigated. The Job's plot titration experiments of the probe BTD with Al^{3+} were first carried out to determine the binding ratio between the probe BTD and Al^{3+}. As shown in Fig. S9,† the maximum fluorescence intensity was obtained when the molar ratio of the probe BTD with Al^{3+} was 0.5, indicating a 1 : 1 metal–ligand chelation ratio between the probe BTD and Al^{3+}. Mass spectrometry analysis was further conducted, as shown in Fig. S10.† The peak at *m*/*z* 565.15 was attributed to $[BTD - Al^{3+} + 2SO_4^{2-} + H^+]^-$ [calcd, *m*/*z*: 564.97]. Moreover, the FT-IR spectra of free probe BTD and the complex of probe BTD and Al^{3+} were obtained, respectively (Fig. S11†). These results further confirmed the binding mode of the probe BTD with Al^{3+}. According to the analyses of Job's plot, ESI-MS and FT-IR spectra, the proposed mechanism for the sensing of Al^{3+} using the probe BTD was reasonable (Scheme 1).

Detection of Al^{3+} in real water samples

To verify whether the probe BTD could detect Al^{3+} ions in real water samples or not, this probe was applied to quantify Al^{3+} ions in Xiangjiang water and tap water. As shown in Table 1, after the addition of 3 μM and 6 μM Al^{3+} ions to different water samples respectively, good results were obtained and the recovery of Al^{3+} ranged from 97.3% to 102.2%. Thus, the probe BTD was suitable to detect Al^{3+} ions in the water samples.

Imaging Al^{3+} in living cells

Encouraged by the aforementioned results, the probe BTD was further applied to the imaging of Al^{3+} in living cells using a laser scanning confocal microscope. According to the results from MTT assays in BEL-7402 cells, the probe BTD has low cytotoxicity towards living cells (Fig. S12†). As shown in Fig. 4, when BEL-7402 cells were incubated with the probe BTD (2.0 μM) for 30 min, a faint green fluorescence was observed (Fig. 4, A1–A3), while, after the addition of Al^{3+} (0.1–0.4 mM), blue fluorescence was observed (Fig. 4, B1–D3). These results indicated that the probe BTD was successfully applied to the imaging of Al^{3+} in living cells.

Imaging of Al^{3+} in zebrafish

Finally, the probe BTD was applied to image Al^{3+} in zebrafish. As shown in Fig. 5, when the zebrafish were treated with the probe BTD (5 μM) for 60 min, a green fluorescence was observed. When the zebrafish was preincubated with Al^{3+} (10, 20, and 50 μM, respectively) and then incubated with the

Table 1 Quantification of Al^{3+} with the probe BTD in real water samples. RSD (%, *n* = 3)

Samples	Al^{3+} (μM)	Spiked (μM)	Detected (μM)	Recovery (%)	RSD (%)
Xiang jiang River	0.00	3.00	2.92	97.3	0.67
		6.00	5.94	99.0	0.52
Tap water	0.00	3.00	2.94	98.0	0.85
		6.00	6.13	102.2	1.23

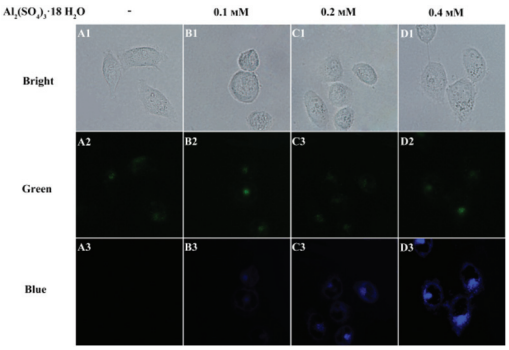

Fig. 4 Confocal fluorescence images of exogenous Al^{3+} in BEL-7402 cells. (A1–D3) The cells were incubated with the probe BTD (2.0 μM) for 30 min and then incubated with 0.1 mM, 0.2 mM and 0.4 mM Al^{3+} for 30 min, respectively. (λ_{ex} = 405 nm, λ_{em} = 421–475 nm for the blue channel; λ_{ex} = 458 nm, λ_{em} = 500–550 nm for the green channel.) Scale bar: 50 μm.

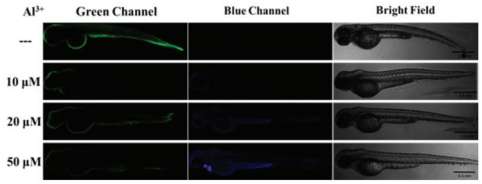

Fig. 5 Confocal fluorescence imaging of exogenous Al^{3+} in zebrafish. Top row: zebrafish were incubated with the probe BTD (5 μM) for 60 min. Others: zebrafish were preincubated with 10, 20 and 50 μM Al^{3+} for 60 min and then incubated with the probe BTD (5 μM) for 60 min, respectively. (λ_{ex} = 405 nm, λ_{em} = 440–500 nm for the blue channel; λ_{ex} = 488 nm, λ_{em} = 510–550 nm for the green channel). Scale bar: 0.5 mm.

probe BTD, a green fluorescence disappeared, and the blue fluorescence was increased. These results demonstrated that the probe BTD is an effective candidate for the monitoring of Al^{3+} fluctuation in zebrafish.

Conclusions

In summary, a novel fluorescent probe BTD for the monitoring of Al^{3+} has been developed based on the AIE mechanism. The probe BTD is easily prepared through a simple three-step process, which could detect Al^{3+} in water samples under mild conditions. And this probe exhibited a fast response, high selectivity, and good sensitivity toward Al^{3+}. Furthermore, the probe BTD was successfully applied to the sensing of Al^{3+} in living cells and zebrafish, which would be helpful for the understanding of the pathological functions of Al^{3+} in biological systems.

Author contributions

Yabing Gan: methodology, investigation, formal analysis, and writing – original draft. Guoxing Yin: investigation and validation. Zhaomin Xu: investigation and validation. Jianhua Wang: conceptualization, methodology, and writing – review & editing. Peng Yin: supervision, conceptualization, funding acquisition, project administration, and writing – review & editing.

Conflicts of interest

There are no conflicts to declare.

Acknowledgements

This work was supported by the funding from the National Natural Science Foundation of China (Grant No. 21877035).

Notes and references

1 E. Delhaize and P. R. Ryan, *Plant Physiol.*, 1995, **107**, 315–321.
2 B. Valeur and I. Leray, *Coord. Chem. Rev.*, 2000, **205**, 3–40.
3 H. Okubo, *Proc. Natl. Acad. Sci. U. S. A.*, 1988, **85**, 3888–3892.
4 S. W. King, J. Savory, M. R. Wills and H. J. Gitelman, *Crit. Rev. Clin. Lab. Sci.*, 1981, **14**, 1–20.
5 I. S. Parkinson, M. K. Ward and D. N. Kerr, *J. Clin. Pathol.*, 1981, **34**, 1285.
6 T. P. Flaten, *Brain Res. Bull.*, 2001, **55**, 187–196.
7 V. K. Gupta, A. K. Jain and G. Maheshwari, *Talanta*, 2007, **72**, 1469–1473.
8 G. D. Fasman, *Coord. Chem. Rev.*, 1996, **149**, 125–165.
9 L. K. Kumawat, N. Mergu, M. Asif and V. K. Gupta, *Sens. Actuators, B*, 2016, **231**, 847–859.
10 Neeraj, A. Kumar, S. K. Asthana, Shweta and K. K. Upadhyay, *J. Photochem. Photobiol., A*, 2016, **329**, 69–76.
11 W. A. Banks and A. J. Kastin, *Neurosci. Biobehav. Rev.*, 1989, **13**, 47–53.
12 V. Rondeau, H. Jacqmin-Gadda, D. Commenges, C. Helmer and J.-F. Dartigues, *Am. J. Epidemiol.*, 2009, **169**, 489–496.
13 M. Frankowski, A. Zioła-Frankowska and J. Siepak, *Talanta*, 2010, **80**, 2120–2126.
14 R. N. Goyal, V. K. Gupta and S. Chatterjee, *Biosens. Bioelectron.*, 2009, **24**, 3562–3568.
15 C.-H. Guo, G.-S. W. Hsu, C.-J. Chuang and P.-C. Chen, *Environ. Toxicol. Pharmacol.*, 2009, **27**, 176–181.
16 H. Wang, Z. Yu, Z. Wang, H. Hao, Y. Chen and P. Wan, *Electroanalysis*, 2011, **23**, 1095–1099.
17 B. J. Sanghavi and A. K. Srivastava, *Analyst*, 2013, **138**, 1395–1404.
18 B. J. Sanghavi, S. Sitaula, M. H. Griep, S. P. Karna, M. F. Ali and N. S. Swami, *Anal. Chem.*, 2013, **85**, 8158–8165.
19 N. S. Gadhari, B. J. Sanghavi and A. K. Srivastava, *Anal. Chim. Acta*, 2011, **703**, 31–40.
20 B. M. Luby, D. M. Charron, C. M. MacLaughlin and G. Zheng, *Adv. Drug Delivery Rev.*, 2017, **113**, 97–121.

21 J. A. Kaczmarski, J. A. Mitchell, M. A. Spence, V. Vongsouthi and C. J. Jackson, *Curr. Opin. Struct. Biol.*, 2019, **57**, 31–38.
22 Y.-J. Liu, F.-F. Tian, X.-Y. Fan, F.-L. Jiang and Y. Liu, *Sens. Actuators, B*, 2017, **240**, 916–925.
23 P. Torawane, K. Tayade, S. Bothra, S. K. Sahoo, N. Singh, A. Borse and A. Kuwar, *Sens. Actuators, B*, 2016, **222**, 562–566.
24 Z. Li, C. Liu, J. Wang, S. Wang, L. Xiao and X. Jing, *Spectrochim. Acta, Part A*, 2019, **212**, 349–355.
25 G. T. Selvan, M. Kumaresan, R. Sivaraj, I. V. M. V. Enoch and P. M. Selvakumar, *Sens. Actuators, B*, 2016, **229**, 181–189.
26 M. Mukherjee, B. Sen, S. Pal, A. Maji, D. Budhadev and P. Chattopadhyay, *Spectrochim. Acta, Part A*, 2016, **157**, 11–16.
27 M. A. Kozlov, D. Y. Uvarov, S. A. Gorbatov, N. G. Kolotirkina, A. D. Averin, V. V. Kachala, K. A. Lyssenko, I. V. Zavarzin and Y. A. Volkova, *Eur. J. Org. Chem.*, 2019, 4196–4206.
28 J.-H. Wang, D.-R. Gao, X.-Y. Wang, Y.-M. Lu, W.-X. Shen and Y.-Y. Lv, *Sens. Actuators, B*, 2019, **294**, 14–23.
29 G. Zhu, Y. Huang, C. Wang, L. Lu, T. Sun, M. Wang, Y. Tang, D. Shan, S. Wen and J. Zhu, *Spectrochim. Acta, Part A*, 2019, **210**, 105–110.
30 S. Mukherjee, P. Mal and H. Stoeckli-Evans, *J. Lumin.*, 2016, **172**, 124–130.
31 L. Bai, F. Tao, L. Li, A. Deng, C. Yan, G. Li and L. Wang, *Spectrochim. Acta, Part A*, 2019, **214**, 436–444.
32 Y. Li, Q. Niu, T. Wei and T. Li, *Anal. Chim. Acta*, 2019, **1049**, 196–212.
33 M. Arduini, F. Felluga, F. Mancin, P. Rossi, P. Tecilla, U. Tonellato and N. Valentinuzzi, *Cheminform*, 2003, **34**, 1606–1607.
34 Y. Hong, J. W. Y. Lam and B. Z. Tang, *Chem. Soc. Rev.*, 2011, **40**, 5361–5388.
35 Y. Liu, Y. Tang, N. N. Barashkov, I. S. Irgibaeva, J. W. Y. Lam, R. Hu, D. Birimzhanova, Y. Yu and B. Z. Tang, *J. Am. Chem. Soc.*, 2010, **132**, 13951–13953.
36 X. Chen, X. Y. Shen, E. Guan, Y. Liu, A. Qin, J. Z. Sun and B. Z. Tang, *Chem. Commun.*, 2013, **49**, 1503–1505.
37 J. Wu, F. Du, P. Zhang, I. A. Khan, J. Chen and Y. Liang, *J. Inorg. Biochem.*, 2005, **99**, 1145–1154.
38 Z. Qiao, Y. Wu, B. Tang, R. Perestrelo and R. Bhalla, *Tetrahedron Lett.*, 2019, **60**, 150918.
39 J. Luo, Z. Xie, J. W. Lam, L. Cheng, H. Chen, C. Qiu, H. S. Kwok, X. Zhan, Y. Liu and D. Zhu, *Chem. Commun.*, 2001, **18**, 1740–1741.
40 Y. Hong, J. W. Y. Lam and B. Z. Tang, *Chem. Commun.*, 2009, **40**, 4332–4353.
41 Y.-J. Tang, S. He, X.-F. Guo and H. Wang, *Analyst*, 2021, **146**, 7740–7747.
42 Y. Ma, W. Gao, L. Zhu, Y. Zhao and W. Lin, *Analyst*, 2020, **145**, 1865–1870.
43 Y. Zhang, Y. Zuo, T. Yang, Z. Gou, X. Wang and W. Lin, *Analyst*, 2019, **144**, 5075–5080.
44 J. Xiong, Z. Li, J. Tan, S. Ji, J. Sun, X. Li and Y. Huo, *Analyst*, 2018, **143**, 4870–4886.
45 M. Ren, L. Wang, X. Lv, Y. Sun, H. Chen, K. Zhang, Q. Wu, Y. Bai and W. Guo, *Analyst*, 2019, **144**, 7457–7462.
46 Q. Wu, L. Feng, J. B. Chao, Y. Wang and S. Shuang, *Analyst*, 2021, **146**, 4348–4356.
47 Z. Liu, X. Zhou, Y. Miao, Y. Hu, N. Kwon, X. Wu and J. Yoon, *Angew. Chem., Int. Ed.*, 2017, **56**, 5812–5816.
48 H. Ren, F. Huo and C. Yin, *New J. Chem.*, 2021, **45**, 9096–9101.
49 W. Zhang, T. Liu, F. Huo, P. Ning, X. Meng and C. Yin, *Anal. Chem.*, 2017, **89**, 8079–8083.
50 T.-B. Ren, S.-Y. Wen, L. Wang, P. Lu, B. Xiong, L. Yuan and X.-B. Zhang, *Anal. Chem.*, 2020, **92**, 4681–4688.
51 Y. Ma, W. Gao, L. Zhu, Y. Zhao and W. Lin, *Chem. Commun.*, 2019, **55**, 11263–11266.
52 X. Liu, X. Gong, J. Yuan, X. Fan, X. Zhang, T. Ren, S. Yang, R. Yang, L. Yuan and X.-B. Zhang, *Anal. Chem.*, 2021, **93**, 5420–5429.
53 Y. Ma, Y. Tang, Y. Zhao and W. Lin, *Anal. Chem.*, 2019, **91**, 10723–10730.